

Encapsulation of Cerium Nitrate within Poly(urea-formaldehyde) Microcapsules for the Development of Self-Healing Epoxy-Based Coating

Gholamali Farzi, Ali Davoodi, Ali Ahmadi, Rasoul Esmaeely Neisiany, Md Khalid Anwer, M. Ali Aboudzadeh

▶ **To cite this version:**

Gholamali Farzi, Ali Davoodi, Ali Ahmadi, Rasoul Esmaeely Neisiany, Md Khalid Anwer, et al.. Encapsulation of Cerium Nitrate within Poly(urea-formaldehyde) Microcapsules for the Development of Self-Healing Epoxy-Based Coating. ACS Omega, 2021, 6, pp.31147 - 31153. 10.1021/acsomega.1c04597 . hal-03515732

HAL Id: hal-03515732

https://univ-pau.hal.science/hal-03515732

Submitted on 6 Jan 2022

HAL is a multi-disciplinary open access archive for the deposit and dissemination of scientific research documents, whether they are published or not. The documents may come from teaching and research institutions in France or abroad, or from public or private research centers.

L'archive ouverte pluridisciplinaire **HAL**, est destinée au dépôt et à la diffusion de documents scientifiques de niveau recherche, publiés ou non, émanant des établissements d'enseignement et de recherche français ou étrangers, des laboratoires publics ou privés.

ACS OMEGA

http://pubs.acs.org/journal/acsodf

Article

Encapsulation of Cerium Nitrate within Poly(urea-formaldehyde) Microcapsules for the Development of Self-Healing Epoxy-Based Coating

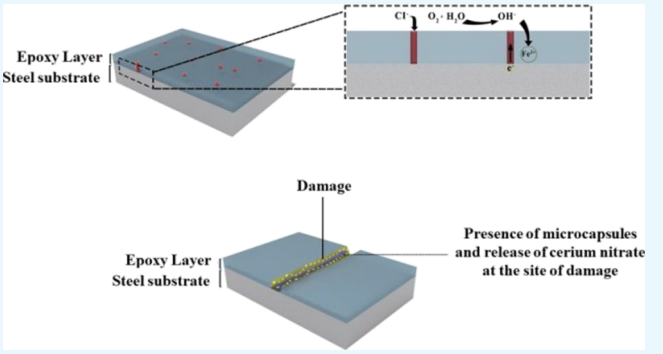
Gholamali Farzi,* Ali Davoodi, Ali Ahmadi, Rasoul Esmaeely Neisiany, Md. Khalid Anwer,* and M. Ali Aboudzadeh*

Cite This: *ACS Omega* 2021, 6, 31147−31153

Read Online

ACCESS | Metrics & More | Article Recommendations

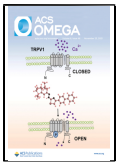
ABSTRACT: In order to study the release of cerium nitrate in a self-healing epoxy-based coating, poly (urea-formaldehyde) (PUF) microcapsules containing cerium nitrate were synthesized. The effects of healing agent concentration and weight percent of microcapsules in the epoxy resin were studied through the incorporation of microcapsules within an epoxy-based coating. The prepared microcapsules were characterized using thermogravimetric analysis and Fourier transform infrared spectroscopy and confirmed the successful encapsulation of cerium nitrate within PUF capsules. The self-healing performance of the prepared epoxy coating was investigated in 0.6 M NaCl solution using electrochemical impedance spectroscopy (EIS) tests. The EIS results indicated the successful release of encapsulated cerium nitrate from PUF microcapsules once the damage occurred in the epoxy coating, which led to effective self-healing of the epoxy-based coating. The presence of chlorine and cerium ions in the solution led to the precipitation of cerium hydroxides and oxides in the scratched area as a passive layer which hindered the corrosion in the damaged area. In addition, the EIS results showed that the healing performance of the coatings depends on the weight percent of microcapsules and the concentration of the self-healing agent. The highest self-healing performance was achieved for the maximum amount of microcapsule incorporation (10 wt %), while the increase in the microcapsule percent led to a decrease in the adhesion of the coating to the substrate.



1. INTRODUCTION

Because of some shortcomings in the barrier performance of the organic coatings, they have been not considered as the tailored barriers. Therefore, any defects caused by chemical and mechanical factors may provide direct access to corrosive agents to the metal surface.[1−4] However, one of the key challenges of the coating technology is how the organic coatings can be formulated for a high-performance anticorrosive system on metal structures. Self-healing systems have been introduced to address the aforementioned shortcomings, while the release of healing agents showed a long-term protective effect.[5−8] The incorporation of self-healing agents in organic coatings leads to a high-performance system with excellent protective properties against mechanical damages and corrosive agents.[9−11] In these systems, after creating environmental damage, they have the ability to recover their initial properties.[12−14] White et al.[15] achieved the first practical demonstration in the field of self-healing materials. Self-healing capabilities were demonstrated by embedding encapsulated dicyclopentadiene as a liquid healing agent into a polymer matrix containing dispersed catalysts. Subsequently, Brown et al.[16] performed a similar work and showed that the agitation rate of the microcapsule preparation step affected the size of the microcapsules. As the agitation rate increases, an emulsion with smaller droplets forms and the average microcapsule diameter decreases.[17−19] In fact, the turbulent fluid flow around the propeller blades controls the size of the microcapsules.[20] Furthermore, the use of ultrasonic waves has a significant effect on the final size of synthesized capsules.[21] Rochmadi and Hasokowati[22] showed that temperature also governs microcapsule size. It was reported that a higher microencapsulation temperature reduces the amount of the microcapsule product. Thus, the microcapsule diameter

Received: August 23, 2021
Accepted: October 27, 2021
Published: November 10, 2021



Downloaded via UNIV OF PAU AND PAYS DE L'ADOUR on January 6, 2022 at 18:56:18 (UTC).
See https://pubs.acs.org/sharingguidelines for options on how to legitimately share published articles.

ACS Publications

© 2021 The Authors. Published by American Chemical Society

distribution shifts to a smaller diameter, and there is a longer microencapsulation time.

Concerning the nature of self-healing materials, researchers have proposed various materials for self-healing coating systems.[7] The corrosion inhibitors have attracted significant attention during these years.[23−26] The passivating and precipitation inhibitors can be used as self-healing agents into microcapsules. Trabelsi et al.[27] added cerium nitrate ($Ce(NO_3)_3$) to silane coating and reported that the barrier properties and the coating resistance of the silane coating significantly improved, while the coating capacitance decreased. The corrosion inhibition of cerium nitrate has been investigated, and it is generally accepted that cerium ions lead to the precipitation of cerium oxides and/or hydroxides that hinder the cathodic reduction reaction of the metallic coatings.[28−30] Therefore, this material can be employed as a highly responsive healing agent in the self-healing performance for organic coatings (i.e., epoxy-based coatings). However, if cerium nitrate is mixed with the epoxy resin before applying on the metallic substrate, it will be consumed over time and could not recover the induced damages during the coating service life. Therefore, its encapsulation is an effective and smart way to keep its functionality longer.

In this paper, cerium nitrate was encapsulated within the poly(urea-formaldehyde) (PUF) microcapsules. PUF was employed as the capsule shell material, and it was considerably investigated in self-healing applications to protect the healing agents due to the facile preparation of PUF microcapsules along with its thermal and chemical stability and compatibility with the epoxy-based matrix.[31−33] The experimental study of self-healing ability in the coating was based on electrochemical impedance spectroscopy (EIS) tests to evaluate the corrosion resistance and self-healing ability of epoxy coatings containing three weight percentages of the microcapsules.

2. RESULTS AND DISCUSSION

2.1. Synthesis of Microcapsules. The microcapsules were synthesized in two steps. The first step comprised urea-formaldehyde pre-polymer synthesis by a polycondensation reaction. While urea-formaldehyde is a gas at room temperature and is soluble in water, its most common use is as a 37% aqueous solution named formalin. Formaldehyde including HCHO monomers shows good polymerization in water. Therefore, by adding a certain amount of urea and formalin under stirring at 70 °C for 1 h, the urea-formaldehyde pre-polymer is synthesized as schematically presented in Figure 1.

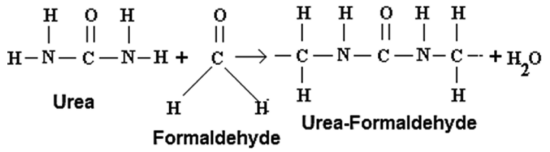


Figure 1. Schematic showing the formation of urea-formaldehyde.

A thermoplastic polymer such as urea-formaldehyde provides a homogeneous dispersion in water at 70 °C. Hence, with the temperature decreasing up to 25 °C, resultant products were in a solid manner. In the second step, which is almost identical to direct emulsion polymerization, the pre-polymer solution was added to distilled water containing polyethylene maleic anhydride (PEMA) as an emulsifier and stabilizer agent under controlled temperature and stirring. Therefore, stirring creates fine bubbles. The prepared PUF particles in the shape of sphere microcapsules formed around the bubbles and solution interfaces.[34] The presence of the emulsifier in the solution resulted in the dispersion of the microcapsules without any sign of aggregations. Figure 2 schematically represents the polymerization process for the microcapsule formation.

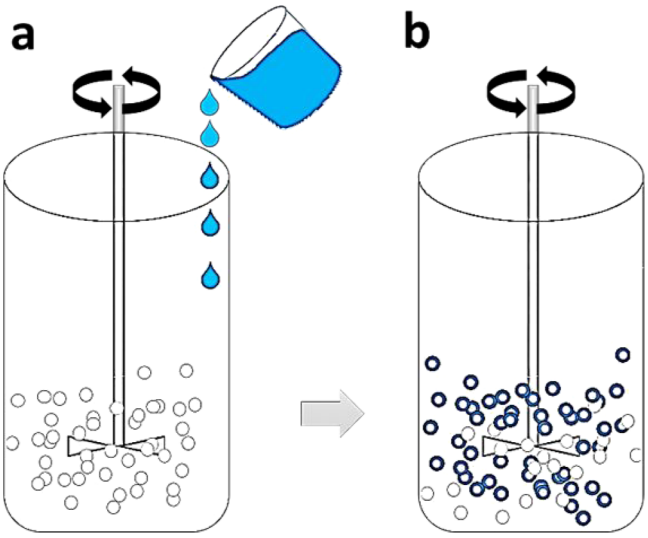


Figure 2. Schematic representation of the microcapsule synthesis: (a) addition of the urea pre-polymer and creation of fine pores and (b) microcapsule formation in the vicinity of the pores.

During the synthesis, three types of microcapsules are created. The microcapsules in the first group have an irregular shape and appear as large aggregated particles at the bottom of the reactor. The microcapsules in the second group, with the average diameters and a quasi-spherical shape, are found in the middle of the reactor and surrounding the propeller blade due to the low possibility of aggregation. The type of microcapsules with small diameters arises at the top of the reactor owing to their light weight. In fact, the turbulence fluid flow near the propeller blade significantly affects the microcapsule size.[20]

The created microcapsules were initially hollow, but because of their thin shells, they will gradually get filled with the solution.[34] Therefore, at the end of the process, the complete drying of the obtained microcapsules requires 2 days at room temperature. During the dry process, the shells of some microcapsules shrunk and finally ruptured due to the evaporation of solvents. Considering the effect of the agitation rate on the size of the obtained microcapsules, which should not be greater than the coating thickness, different agitation rates were examined to appraise the optimum rate of 1450−1500 rpm.

2.2. Characterization of Microcapsules. Since the majority of the microcapsules are filled with the solution, it can be expected that $Ce(NO_3)_3$ in water can enter the microcapsules and fill them. The presence of $Ce(NO_3)_3$ was confirmed by thermogravimetric analysis (TGA) and Fourier transform infrared spectroscopy (FTIR) tests. As can be seen in Figure 3, at about 100 °C, the hollow microcapsules had a slight weight loss due to the residual moisture. At about 240 °C, the hollow microcapsules underwent a steep weight loss, which may be attributed to the thermal decomposition temperature of the cross-linked PUF polymer. For micro-

https://doi.org/10.1021/acsomega.1c04597
ACS Omega 2021, 6, 31147−31153

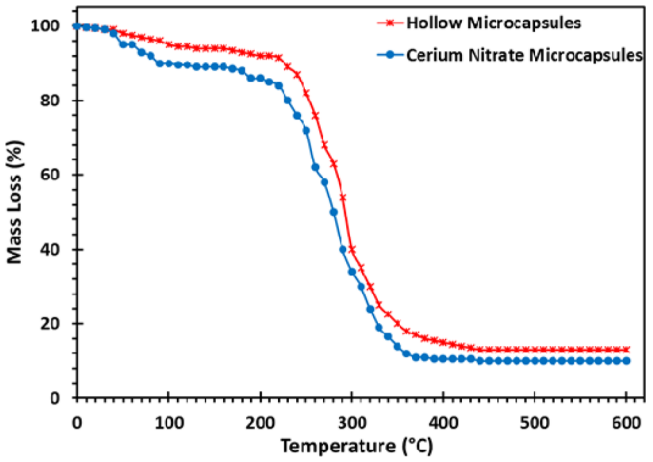


Figure 3. TGA curves of PUF microcapsules with/without cerium nitrate.

capsules containing $Ce(NO_3)_3$, the 8% weight loss of microcapsules at temperatures between 50 and 90 °C occurred due to not only the removal of moisture and crystal water but also the formation of oxide compounds from $Ce(NO_3)_3$. At a higher temperature, after the first weight loss, both the TGA curves of the microcapsules had the same thermal decomposition behavior since $Ce(NO_3)_3$ evaporated and only the PUF shell remained.

The synthesis of PUF microcapsules and the presence of $Ce(NO_3)_3$ in them were also confirmed by FTIR tests, and the obtained results are shown in Figure 4. The identified peaks of

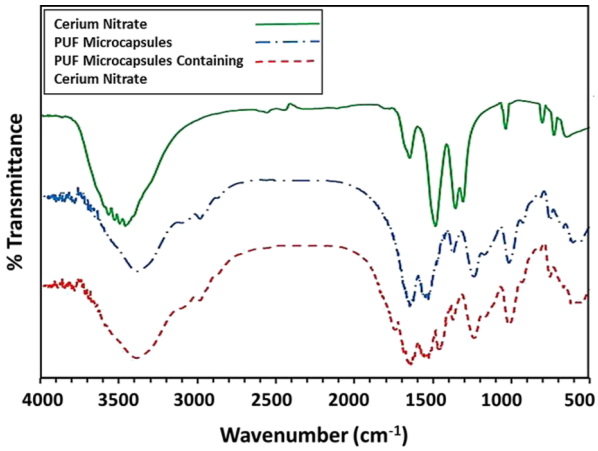


Figure 4. FTIR spectra of PUF microcapsules.

PUF microcapsules with or without $Ce(NO_3)_3$ are at about 1550 cm^{-1} (N−H), 1640 cm^{-1} (C═O), and 3330−3350 cm^{-1} (N−H, O−H).[35] In addition, as can be seen in FTIR curves of the microcapsules containing $Ce(NO_3)_3$, the characteristics peaks at 1390 and 1600 cm^{-1} are associated with the presence of $Ce(NO_3)_3$,[36] which confirms the successful encapsulation of $Ce(NO_3)_3$ within PUF microcapsules.

2.3. Effect of Microcapsule Incorporation on Adhesion Strength of the Coating. The results of adhesion test coatings are listed in Table 1. The adhesion strength of the coatings decreased as the capsule concentrations increased. The results showed that the control sample (without capsules) had the highest adhesion in the coatings. In fact, the existence of microcapsules as an external agent into the polymer coating

Table 1. Results of the Adhesion Test

coatings	coat. A	coat. B	coat. C	coat. D
quality[a]	4	3	3	3

[a]The adhesion quality of the coatings was determined according to the Figure 1 of ASTM D3350.

caused the discontinuity and consequently reduction of contact area between the substrate and the coating.[37,38]

2.4. Corrosion Resistance Evaluation. To assess the self-healing performance of the coatings, the EIS tests[39] were performed on the scratched epoxy coatings in 0.6 M NaCl solution. Figure 5 shows the Bode results of the coatings after 1 day and a week of immersion. The control coating (without microcapsules) showed almost the same final resistance. Considering the existence of scratches in the coating and also large amounts of Cl^- in electrolyte solutions, the corrosion process in the scratched area increases. Since the time of electrolyte penetration into organic coatings is long, the corrosion at the beginning of the immersion developed from scratched areas. Due to the small size of the scratched areas, the corrosion products in this area are accumulated, leading to a decrease in the corrosion process during a week. Incorporating microcapsules containing $Ce(NO_3)_3$ to the epoxy resin however led to the creation of fine bubbles in the epoxy resin and especially around microcapsules. Therefore, after coating the plate and drying the coatings, these bubbles ruptured and remained in the form of fine pores in microcapsules and the epoxy resin interface. Therefore, the increase in microcapsule content influenced the final resistance of the coatings, that is, a decrease in the corrosion resistance. However, the existence of $Ce(NO_3)_3$ contained microcapsules in different amounts in the coatings resulted in significant differences in the coating corrosion resistance. Since coating D contained the highest amount of $Ce(NO_3)_3$, it showed the best self-healing performance associated with the highest corrosion resistance after scratch in the coating and immersion.

The interpretation of the obtained EIS results can be made by numerical fitting using the equivalent circuits depicted in Figure 6. In this equivalent circuit, constant phase elements (CPEs) were used instead of pure capacitors. Accordingly, in the fitted equivalent circuit of the coating, two capacitive responses are observed, including those of the epoxy resin, C_{1coat}, and the dispersed PUF microcapsules in the resin, C_{2coat}. Therefore, at high frequencies, the resistance and capacitive response of the epoxy resin (R_{1C}, CPE_{1C}) are observed; at medium frequencies, the resistance and capacitive response of PUF microcapsules (R_{2C}, CPE_{2C}) are observed; and at low frequencies, the resistance and capacitive response of the substrate (R_P, CPE_{dl}) are observed.

The evolution of the different electrochemical parameters versus time, defined by the equivalent circuits, is presented in Figure 7. The high amount of R_{1C} in coating D is due to the presence of a high percentage of PUF microcapsules. The high volume/weight ratio of microcapsules in coating D blocked the pores. In other words, pathways for electrolyte penetration are blocked. In addition, a high amount of R_{2C} is available because of the high percentage of microcapsules in coating D. The high amount of $Ce(NO_3)_3$ in coating D causes more release of Ce^{+3} and Ce^{+4} ions. These ions are at a close distance from the substrate in the electrical double layer in the steel and electrolyte solution interface. Furthermore, the coating D CPE diagram versus time confirms the R_P data. The presence of Cl^-

https://doi.org/10.1021/acsomega.1c04597
ACS Omega 2021, 6, 31147−31153

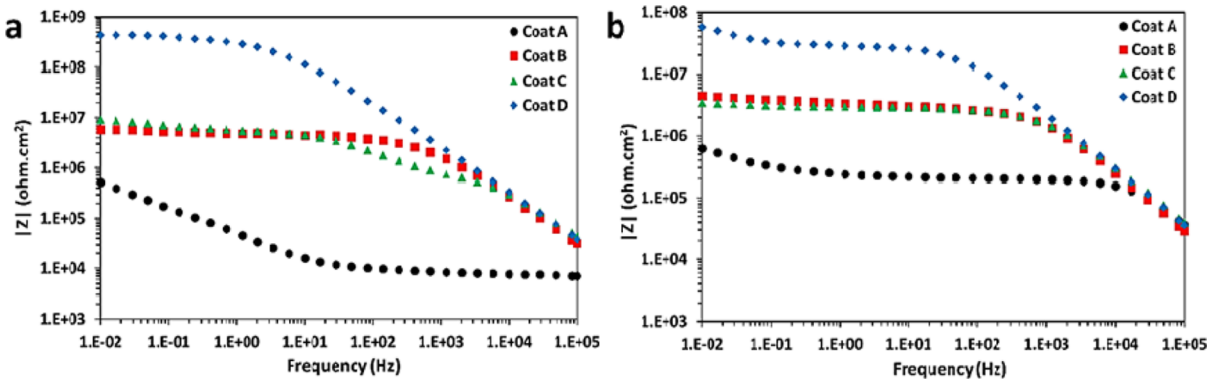


Figure 5. Bode plot corresponding to the epoxy coating with different amounts of cerium nitrate microcapsules after (a) 1 day and (b) 7 days of immersion in 0.6 M NaCl.

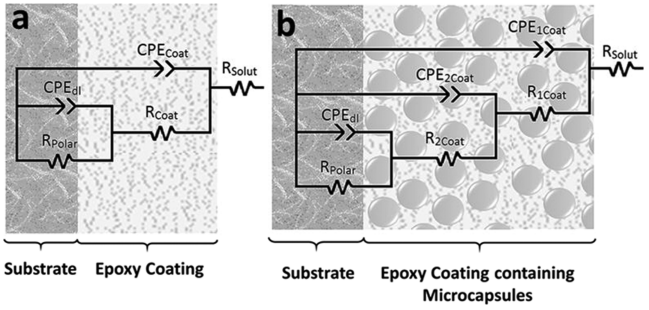


Figure 6. Equivalent circuits used for numerical fitting of the EIS data for (a) coating A and (b) coatings B, C, and D.

ions in the solution and Ce^{+3} and Ce^{+4} ions leads to the precipitation of cerium hydroxides and oxides in the scratched area, which hinders the corrosion in areas.[27,30] After 1 week, more ions precipitated in the scratched area, which consequently filled up the scratched area and provided a healing layer. Aramaki showed that cerium nitrate produces Ce^{+3} and Ce^{+4} when it solutes in the water and encounters Cl^- ions[28,29]

$$Ce(NO_3)_3 \cdot 6H_2O + H_2O \rightarrow Ce^{+3} + 3NO_3^- + 7H_2O \quad (1)$$

$$Ce^{+3} \xrightarrow{Cl^-} Ce^{+4} \quad (2)$$

Consequently, Ce^{+3} and Ce^{+4} produce cerium oxide

$$Ce^{+4} + 2H_2O \rightarrow CeO_2 + 4H^+ \quad (3)$$

The produced cerium hydroxide also then precipitates to cerium oxide according to the following equation:

$$Ce(OH)_4 \rightarrow CeO_2 + 2H_2O \quad (4)$$

Figure 8 shows the images of the scratched areas in the coatings. Coating D containing 10% wt of $Ce(NO_3)_3$ PUF microcapsules had the best healing performance in the scratched area. These images perfectly confirm the EIS results.

3. CONCLUSIONS

Cerium nitrate was successfully encapsulated within PUF microcapsules through a two-step polymerization process. TGA and FTIR results confirmed the existence of $Ce(NO_3)_3$ in PUF microcapsules. The obtained results of the adhesion test on the coatings showed that the existence of microcapsules resulted in the discontinuity and reduction in the adhesion of the coating to the metallic substrate; however, the coating containing microcapsules showed the self-healing ability after damage and encountering corrosive ions. The presence of chlorine and cerium ions in the solution leads to the precipitation of cerium hydroxides and oxides in the scratched area as a passive layer, which hinders the corrosion in the damaged area. In addition, the coatings containing 10 wt % of microcapsules showed the best healing performance due to more available cerium nitrate at the damaged sites for healing performance along with blocking of the pathways for electrolyte penetration due to the high volume/weight ratio of microcapsules in the epoxy-based matrix.

4. MATERIALS AND METHODS

4.1. Materials. Commercial epoxy bisphenol A and the polyamine hardener were purchased from Mokarrar Company (Tehran, Iran) and used as received as a commercial epoxy-based coating. Urea, formalin (37% formaldehyde in water), ethanol, acetone, formic acid, cerium nitrate hexahydrate, sodium chloride, and poly(ethylene-*g*-maleic anhydride) (PEMA) powder (with average M_w = 100−500 g·mol^{-1}) were all purchased from Sigma-Aldrich.

4.2. Synthesis of Microcapsules. Hollow microcapsules were prepared by a polycondensation reaction of the urea-formaldehyde pre-polymer on the surface of entrained air bubbles in a reaction vessel based on the method reported by Jin et al.[34] The hollow microcapsules were synthesized in two steps. In the first step, a pre-polymer solution was prepared by dissolving 10.25 g of urea into 27.5 g of formaldehyde solution (37%) in a 250 mL beaker. The reaction proceeded at 70 °C for 1 h. In the second stage, the pre-polymer solution was added to a double-walled glass reactor which contains 50 mL of distilled water and 12.55 mL of 5 wt % PEMA, while the temperature was controlled at 30 °C. Subsequently, the pre-polymer solution was agitated with a three-bladed mechanical mixer at 1450 rpm. The propeller was placed just beneath the solution's surface in order to entrap air bubbles. The bath temperature was kept at 30 °C, and the pH was adjusted at 2.0 using a few drops of formic acid. Once the bath temperature reached 34 °C, 25 mL of warm distilled water (ca. 30 °C) was added. Followed by 15 min intervals, sequentially, 15, 15, 50, and 50 mL of hot distilled water were added. The solution was allowed to react for 2 h, while the water bath temperature was set at 34 °C. The hollow microcapsules between 50 and 160 μm were obtained and measured using a sieving device.

https://doi.org/10.1021/acsomega.1c04597
ACS Omega 2021, 6, 31147−31153

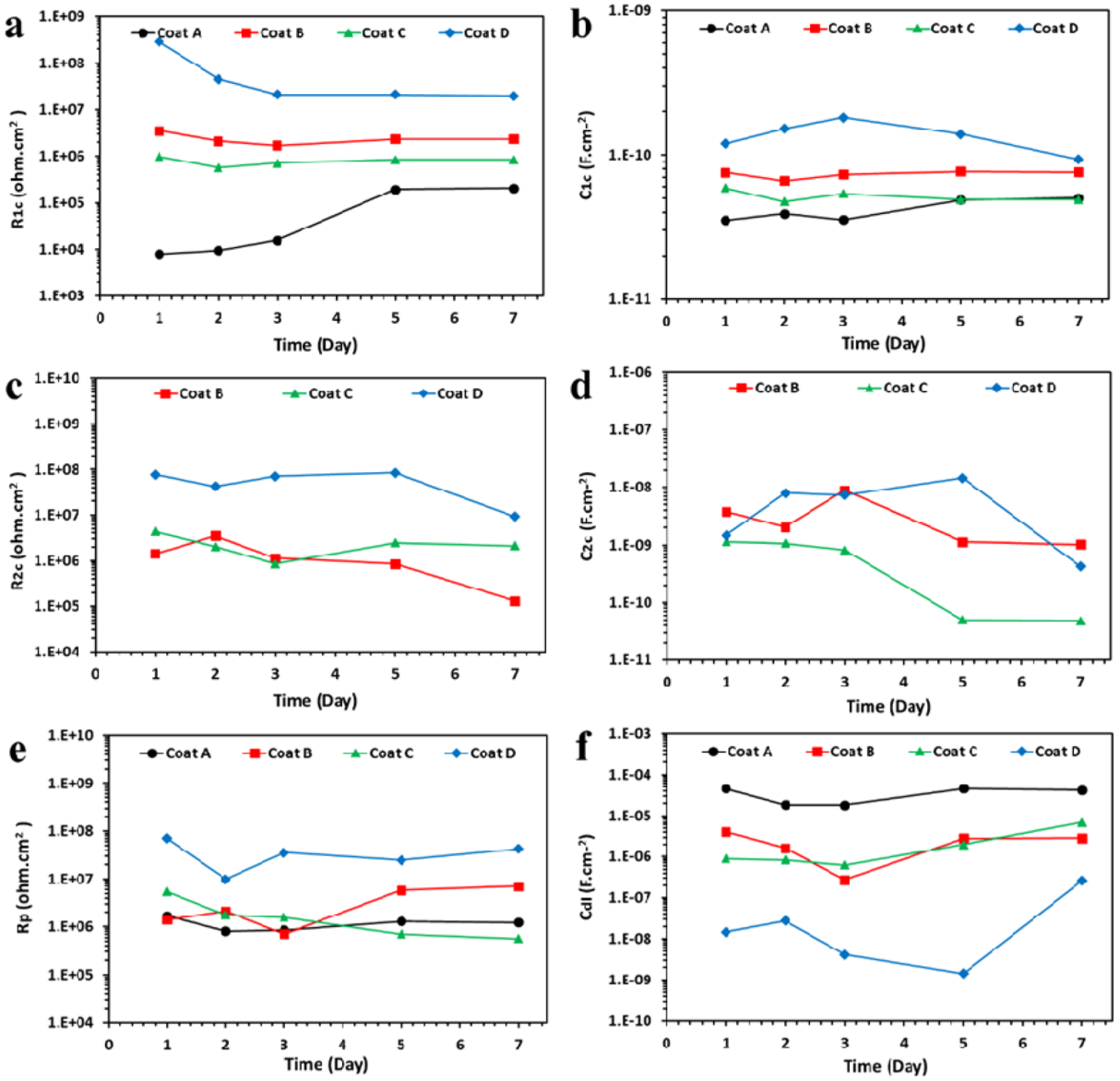


Figure 7. EIS results of the artificially scratched coatings during the immersion period: (a) R_{1C}, (b) C_{1c}, (c) R_{2c}, (d) C_{2C}, (e) R_p, and (f) C_{dl}.

The synthesis of microcapsules containing $Ce(NO_3)_3$ was similar to the synthesis of hollow microcapsules except in the second stage of the synthesis, and the pre-polymer solution was added to 50 mL of distilled water, 12.55 mL of 5 wt % PEMA, and 10 mL of 5 wt % $Ce(NO_3)_3$ aqua solution. The synthesized microcapsules were slightly larger than the hollow ones, and their average size was measured to be between 75 and 180 μm.

4.3. Preparation of Coatings. Commercial carbon steel plates with dimensions of 160 mm × 100 mm and a thickness of 0.5 mm were used as a substrate. The plates were prepared by grinding with an 800-grit emery paper in the final stage and then washing with acetone and drying with a hot blow of air. Self-healing coatings were prepared by dispersing three different percentages of the synthesized $Ce(NO_3)_3$ microcapsules into the epoxy resin at ambient temperature, followed by mixing with the hardener just before applying to the metallic substrate. The resins containing microcapsules were applied on steel using a precise micrometer adjustable film applicator. The coating thickness was initially adjusted to 300 μm using the wet film applicator, and then, the thickness of the dry films was evaluated using a CM880FN coating thickness gauge for the cured coatings at ambient temperature for 1 week. The thicknesses of dried coatings are summarized in Table 2. A pure epoxy coating sample was also prepared under similar conditions and used as a reference. Nomenclatures of the coatings are shown in Table 2.

4.4. Characterizations. *4.4.1. Characterization of the Prepared Microcapsules.* The prepared microcapsules were characterized by TGA tests using a NETZSCH instrument under nitrogen gas and a heating rate of 10 °C/min. In addition, the FTIR tests were performed for the neat cerium nitrate, empty PUF microcapsules, and microcapsules containing using a Shimadzu 4800S device.

4.4.2. Adhesion of the Coatings. In order to evaluate the effect of microcapsule incorporation on the adhesion of the coatings, the adhesion tests were performed according to standards D3330 and D3359. Vertical and parallel lines on the coating are created using Cross-Cut tools. Then, the scratched area is cleaned using a brush. A 75 mm and wide

https://doi.org/10.1021/acsomega.1c04597
ACS Omega 2021, 6, 31147−31153

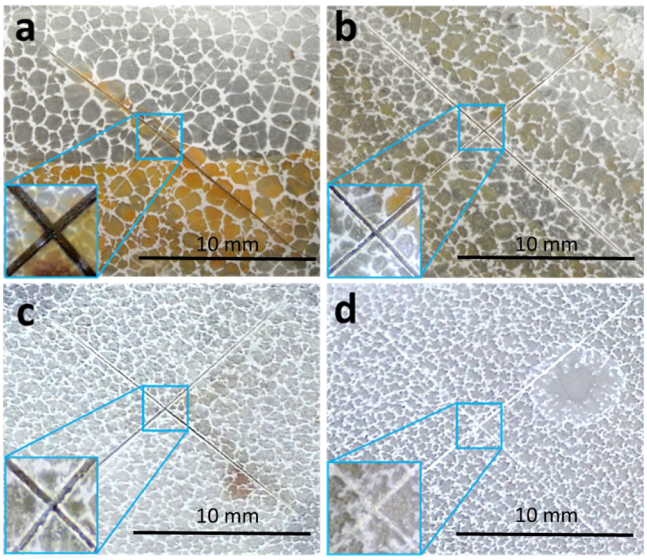


Figure 8. Optical microscopy images of coatings (a) A, (b) B, (c) C, and (d) D after 7 day immersion in 0.6 M NaCl solution.

Table 2. Nomenclatures Used in the Present Study for Epoxy Coatings

denoted as	composition of the epoxy coating containing microencapsulated $Ce(NO_3)_3$ in the PUF shell (wt %)	dry film thickness (μm)
A		170
B	2.5	183
C	5	185
D	10	189

semitransparent pressure-sensitive tape is placed on the grid patterns and pressured to ensure enough contact between the tape and coating. The tape was then removed with a steady motion by pulling at a 180° angle. The tape and the scratched area on the coating are then evaluated according to the standard table.

4.4.3. Corrosion Resistance Evaluation. To investigate the self-healing performance of the coatings, the cross-cut coating samples were prepared according to ASTM D1654 using a razor blade with a length of 2 cm, and the EIS tests were then carried out using Ivium Technologies equipped by a Faraday cage at room temperature. The experiments were achieved in a conventional three-electrode electrochemical cell equipped with a Pt counter electrode, saturated calomel as the reference electrode, and specimens as the working electrode. The measured frequencies ranged from 100 kHz down to 10−2 Hz. Electrochemical experiments were performed during sample immersion in 0.6 M NaCl three times, bringing about the same result each time.

AUTHOR INFORMATION

Corresponding Authors

Gholamali Farzi − *Department of Materials and Polymer Engineering, Faculty of Engineering, Hakim Sabzevari University, Sabzevar 9617976487, Iran;* orcid.org/0000-0002-6629-6743; Email: alifarzi@yahoo.com

Md. Khalid Anwer − *Department of Pharmaceutics, College of Pharmacy, Prince Sattam Bin Abdulaziz University, Alkharj 11942, Saudi Arabia*; Email: mkanwer2002@yahoo.co.in

M. Ali Aboudzadeh − *CNRS, University Pau & Pays Adour, E2S UPPA, Institut des Sciences Analytiques et de Physico-Chimie pour l'Environnement et les Matériaux, IPREM, UMR5254, Pau 64000, France;* orcid.org/0000-0001-8829-8072; Email: m.aboudzadeh-barihi@univ-pau.fr

Authors

Ali Davoodi − *Materials and Metallurgical Engineering Department, Faculty of Engineering, Ferdowsi University of Mashhad, Mashhad 917751111, Iran*

Ali Ahmadi − *Department of Materials and Polymer Engineering, Faculty of Engineering, Hakim Sabzevari University, Sabzevar 9617976487, Iran*

Rasoul Esmaeely Neisiany − *Department of Materials and Polymer Engineering, Faculty of Engineering, Hakim Sabzevari University, Sabzevar 9617976487, Iran;* orcid.org/0000-0002-6988-3898

Complete contact information is available at: https://pubs.acs.org/10.1021/acsomega.1c04597

Funding

This research received no external funding.

Notes

The authors declare no competing financial interest.

ACKNOWLEDGMENTS

This work was supported by Hakim Sabzevari University.

REFERENCES

(1) McCafferty, E. Corrosion Under Organic Coatings. *Introduction to Corrosion Science*; McCafferty, E., Ed.; Springer New York: New York, NY, 2010; pp 403−425.

(2) Ding, Y.; Zhong, J.; Xie, P.; Rong, J.; Zhu, H.; Zheng, W.; Wang, J.; Gao, F.; Shen, L.; He, H.; Cheng, Z. Protection of Mild Steel by Waterborne Epoxy Coatings Incorporation of Polypyrrole Nanowires/Graphene Nanocomposites. *Polymers* **2019**, *11*, 1998.

(3) Wen, J.-G.; Geng, W.; Geng, H.-Z.; Zhao, H.; Jing, L.-C.; Yuan, X.-T.; Tian, Y.; Wang, T.; Ning, Y.-J.; Wu, L. Improvement of Corrosion Resistance of Waterborne Polyurethane Coatings by Covalent and Noncovalent Grafted Graphene Oxide Nanosheets. *ACS Omega* **2019**, *4*, 20265−20274.

(4) Malekkhouyan, R.; Neisiany, R. E.; Khorasani, S. N.; Das, O.; Berto, F.; Ramakrishna, S. The influence of size and healing content on the performance of extrinsic self-healing coatings. *J. Appl. Polym. Sci.* **2021**, *138*, 49964.

(5) Liu, J.; Cao, J.; Zhou, Z.; Liu, R.; Yuan, Y.; Liu, X. Stiff Self-Healing Coating Based on UV-Curable Polyurethane with a "Hard Core, Flexible Arm" Structure. *ACS Omega* **2018**, *3*, 11128−11135.

(6) Koochaki, M. S.; Khorasani, S. N.; Neisiany, R. E.; Ashrafi, A.; Trasatti, S. P.; Magni, M. A highly responsive healing agent for the autonomous repair of anti-corrosion coatings on wet surfaces. In operando assessment of the self-healing process. *J. Mater. Sci.* **2021**, *56*, 1794−1813.

(7) Wang, S.; Urban, M. W. Self-healing polymers. *Nat. Rev. Mater.* **2020**, *5*, 562−583.

(8) Aboudzadeh, M. A.; Zhu, H.; Pozo-Gonzalo, C.; Shaplov, A. S.; Mecerreyes, D.; Forsyth, M. Ionic conductivity and molecular dynamic behavior in supramolecular ionic networks; the effect of lithium salt addition. *Electrochim. Acta* **2015**, *175*, 74−79.

(9) Odarczenko, M.; Thakare, D.; Li, W.; Yang, K.; Tang, S.; Venkateswaran, S. P.; Sottos, N. R.; White, S. R. Self-Protecting Epoxy Coatings with Anticorrosion Microcapsules. *ACS Omega* **2018**, *3*, 14157−14164.

(10) Fadl, A. M.; Abdou, M. I.; Hamza, M. A.; Sadeek, S. A. Corrosion-inhibiting, self-healing, mechanical-resistant, chemically

and UV stable PDMAS/TiO2 epoxy hybrid nanocomposite coating for steel petroleum tanker trucks. *Prog. Org. Coat.* **2020**, *146*, 105715.
(11) Šobak, M.; Štular, D.; Štirn, Ž.; Žitko, G.; Čelan Korošin, N.; Jerman, I. Influence of the Prepolymer Type and Synthesis Parameters on Self-Healing Anticorrosion Properties of Composite Coatings Containing Isophorone Diisocyanate-Loaded Polyurethane Microcapsules. *Polymers* **2021**, *13*, 840.
(12) Rezvani Ghomi, E.; Esmaeely Neisiany, R.; Nouri Khorasani, S.; Dinari, M.; Ataei, S.; Koochaki, M. S.; Ramakrishna, S. Development of an epoxy self-healing coating through the incorporation of acrylic acid-co-acrylamide copolymeric gel. *Prog. Org. Coat.* **2020**, *149*, 105948.
(13) Safdari, A.; Khorasani, S. N.; Neisiany, R. E.; Koochaki, M. S. Corrosion Resistance Evaluation of Self-Healing Epoxy Coating Based on Dual-Component Capsules Containing Resin and Curing Agent. *Int. J. Polym. Sci.* **2021**, *2021*, 6617138.
(14) Panahi, P.; Khorasani, S. N.; Koochaki, M. S.; Dinari, M.; Das, O.; Neisiany, R. E. Synthesis of Cloisite 30B-acrylamide/acrylic acid nanogel composite for self-healing purposes. *Appl. Clay Sci.* **2021**, *210*, 106174.
(15) White, S. R.; Sottos, N. R.; Geubelle, P. H.; Moore, J. S.; Kessler, M. R.; Sriram, S. R.; Brown, E. N.; Viswanathan, S. Autonomic healing of polymer composites. *Nature* **2001**, *409*, 794−797.
(16) Brown, E. N.; Kessler, M. R.; Sottos, N. R.; White, S. R. In situ poly (urea-formaldehyde) microencapsulation of dicyclopentadiene. *J. Microencapsul.* **2003**, *20*, 719−730.
(17) Caruso, M. M.; Blaiszik, B. J.; Jin, H.; Schelkopf, S. R.; Stradley, D. S.; Sottos, N. R.; White, S. R.; Moore, J. S. Robust, Double-Walled Microcapsules for Self-Healing Polymeric Materials. *ACS Appl. Mater. Interfaces* **2010**, *2*, 1195−1199.
(18) Huang, M.; Zhang, H.; Yang, J. Synthesis of organic silane microcapsules for self-healing corrosion resistant polymer coatings. *Corros. Sci.* **2012**, *65*, 561−566.
(19) Khorasani, S. N.; Ataei, S.; Neisiany, R. E. Microencapsulation of a coconut oil-based alkyd resin into poly(melamine−urea−formaldehyde) as shell for self-healing purposes. *Prog. Org. Coat.* **2017**, *111*, 99−106.
(20) Zhao, Y.; Zhang, W.; Liao, L.-p.; Wang, S.-j.; Li, W.-j. Self-healing coatings containing microcapsule. *Appl. Surf. Sci.* **2012**, *258*, 1915−1918.
(21) Samadzadeh, M.; Boura, S. H.; Peikari, M.; Kasiriha, S. M.; Ashrafi, A. A review on self-healing coatings based on micro/nanocapsules. *Prog. Org. Coat.* **2010**, *68*, 159−164.
(22) Rochmadi, A. P.; Hasokowati, W. Mechanism of micro-encapsulation with urea-formaldehyde polymer. *Am. J. Appl. Sci.* **2010**, *7*, 739−745.
(23) Selvakumar, N.; Jeyasubramanian, K.; Sharmila, R. Smart coating for corrosion protection by adopting nano particles. *Prog. Org. Coat.* **2012**, *74*, 461−469.
(24) Jadhav, R. S.; Mane, V.; Bagle, A. V.; Hundiwale, D. G.; Mahulikar, P. P.; Waghoo, G. Synthesis of multicore phenol formaldehyde microcapsules and their application in polyurethane paint formulation for self-healing anticorrosive coating. *Int. J. Ind. Chem.* **2013**, *4*, 31.
(25) Siva, T.; Sathiyanarayanan, S. Self healing coatings containing dual active agent loaded urea formaldehyde (UF) microcapsules. *Prog. Org. Coat.* **2015**, *82*, 57−67.
(26) Hasanzadeh, M.; Shahidi, M.; Kazemipour, M. Application of EIS and EN techniques to investigate the self-healing ability of coatings based on microcapsules filled with linseed oil and CeO2 nanoparticles. *Prog. Org. Coat.* **2015**, *80*, 106−119.
(27) Trabelsi, W.; Cecilio, P.; Ferreira, M. G. S.; Montemor, M. F. Electrochemical assessment of the self-healing properties of Ce-doped silane solutions for the pre-treatment of galvanised steel substrates. *Prog. Org. Coat.* **2005**, *54*, 276−284.
(28) Aramaki, K. Self-healing protective films prepared on zinc by treatments with cerium (III) nitrate and sodium phosphate. *Corros. Sci.* **2002**, *44*, 2621−2634.
(29) Aramaki, K. Preparation of chromate-free, self-healing polymer films containing sodium silicate on zinc pretreated in a cerium (III) nitrate solution for preventing zinc corrosion at scratches in 0.5 M NaCl. *Corros. Sci.* **2002**, *44*, 1375−1389.
(30) Heakal, F. E.-T.; Shehata, O. S.; Tantawy, N. S. Enhanced corrosion resistance of magnesium alloy AM60 by cerium (III) in chloride solution. *Corros. Sci.* **2012**, *56*, 86−95.
(31) Lang, S.; Zhou, Q. Synthesis and characterization of poly(urea-formaldehyde) microcapsules containing linseed oil for self-healing coating development. *Prog. Org. Coat.* **2017**, *105*, 99−110.
(32) Zotiadis, C.; Patrikalos, I.; Loukaidou, V.; Korres, D. M.; Karantonis, A.; Vouyiouka, S. Self-healing coatings based on poly(urea-formaldehyde) microcapsules: In situ polymerization, capsule properties and application. *Prog. Org. Coat.* **2021**, *161*, 106475.
(33) Ismail, N. A.; Khan, A.; Fayyad, E.; Kahraman, R.; Abdullah, A. M.; Shakoor, R. A. Self-Healing Performance of Smart Polymeric Coatings Modified with Tung Oil and Linalyl Acetate. *Polymers* **2021**, *13*, 1609.
(34) Jin, H.; Mangun, C. L.; Stradley, D. S.; Moore, J. S.; Sottos, N. R.; White, S. R. Self-healing thermoset using encapsulated epoxy-amine healing chemistry. *Polymer* **2012**, *53*, 581−587.
(35) Zhang, C.; Wang, H.; Zhou, Q. Preparation and characterization of microcapsules based self-healing coatings containing epoxy ester as healing agent. *Prog. Org. Coat.* **2018**, *125*, 403−410.
(36) Ghamami, S.; Kazemzade Anari, S.; Bakhshi, M.; Lashgari, A.; Salgado-Morán, G.; Glossman-Mitnik, D. Preparation and Characterization of Cerium (III) Doped Captopril Nanoparticles and Study of their Photoluminescence Properties. *Open Chem.* **2016**, *14*, 60−64.
(37) Hatami Boura, S.; Peikari, M.; Ashrafi, A.; Samadzadeh, M. Self-healing ability and adhesion strength of capsule embedded coatings—Micro and nano sized capsules containing linseed oil. *Prog. Org. Coat.* **2012**, *75*, 292−300.
(38) Malekkhouyan, R.; Nouri Khorasani, S.; Esmaeely Neisiany, R.; Torkaman, R.; Koochaki, M. S.; Das, O. Preparation and Characterization of Electrosprayed Nanocapsules Containing Coconut-Oil-Based Alkyd Resin for the Fabrication of Self-Healing Epoxy Coatings. *Appl. Sci.* **2020**, *10*, 3171.
(39) Thiangpak, P.; Rodchanarowan, A. Self-Healing Abilities of Shape-Memory Epoxy-Contained Polycaprolactone Microspheres Filled with Cerium(III) Nitrate Coated on Aluminum 2024-T3. *ACS Omega* **2020**, *5*, 25647−25654.

https://doi.org/10.1021/acsomega.1c04597
ACS Omega 2021, 6, 31147−31153